Global stability of spherical polytropes

Henry E. Kandrup,*,† M. Elaine Mahon,†,‡ and Haywood Smith, Jr.§
Department of Astronomy, University of Florida, Gainesville, Florida 32611
(Received 8 November 1993)

Recently, it has been proved that the spherical polytropes are globally stable solutions to the collisionless Boltzmann, or Vlasov, equation of galactic dynamics. This proof provides a partial explanation of the results of numerical simulations of colliding polytropes described herein, which show that these objects are indeed extremely robust.

PACS number(s): 05.20.Dd, 98.10.+z

The numerical experiments summarized here involved zero impact parameter encounters of two spherical polytropes with the same polytropic index n, each comprised of $N_{\rm tot}=2000$ identical particles. As discussed, e.g., in [1], polytropes are time-independent solutions to the Vlasov-Poisson, or collisionless Boltzmann, equation, characterized by a one-particle distribution function

$$f_0(\mathbf{r},\mathbf{v})=\begin{cases}\text{const}\times(E_0-E)^{n-3/2} & \text{if } E\le 0\\ 0 & \text{if } E>0\end{cases},$$

where $E=v^2/2+\Phi[f_0]$ denotes the energy of a unit mass test particle with velocity $\mathbf{v}$ moving in the self-consistent potential $\Phi(\mathbf{r})$ associated with the equilibrium distribution f_0. The constant $E_0=\Phi_0$ denotes the value of the potential at the boundary of the system, where the spatial density $\rho\to 0$. The potential is so normalized that $\Phi\to 0$ as $\mathbf{r}\to\infty$. For $\frac{1}{2}<n\le 5$, this distribution gives rise to a collisionless equilibrium with an everywhere finite mass density and a finite total mass. It is well known [2] that, for $n>\frac{3}{2}$, these equilibria constitute linearly stable solutions to the Vlasov-Poisson system; and, as has been shown recently by Aly [3], these equilibria are nonlinearly stable as well.

Theory has less to say about the stability of polytropes with $n\le\frac{3}{2}$, since the aforementioned proof of stability requires that df_0/dE be everywhere negative. Violating the condition $df_0/dE<0$ implies an "energetic" instability in the sense that there exist dynamically accessible perturbations that decrease the energy of the equilibrium, but this does not necessarily imply a linear instability [4]. Indeed, numerical simulations, e.g., by Hénon [5], indicate that these polytropes behave stably down to a value very close to the limiting $n=\frac{1}{2}$.

In these experiments, each polytrope constituted a different random microscopic realization of a macroscopic object constrained to have an initial radius $R_0=1.0$. Four different experiments were performed, corresponding to pairs of identical polytropes with polytropic indices $n=1$, 2, 3, and 4. In each case, the two polytropes were originally separated by a distance $r=3$. The initial relative velocities were so chosen that, extrapolated to when the two polytropes were infinitely far apart, their relative velocity $v_{\rm rel}=3v_{\rm rms}$, with $v_{\rm rms}$ the rms velocity of the particles within an individual polytrope.

The specified initial data were evolved forward in time using a direct N-body code which solved the coupled equations of motion for all 4000 particles. The particles were assumed to interact via forces derived from a softened two-body potential

$$V_{ij}=-\frac{Gm}{(\mathbf{r}_{ij}^2+\epsilon^2)^{1/2}},$$

with $\mathbf{r}_{ij}\equiv\mathbf{r}_i-\mathbf{r}_j$ and ϵ a softening parameter that effectively legislates a minimum impact parameter for close encounters. All the simulations involved the choice $\epsilon=10^{-2}$. Previous numerical experiments [6] showed that this value is sufficiently large that, for the duration of the run, the evolution should be essentially collisionless. This duration was $\sim(15-25)t_{\rm cr}$, where $t_{\rm cr}\approx(r_0^3/2GN_{\rm tot}m)^{1/2}$ denotes a characteristic dynamical, or crossing, time for an individual polytrope, defined in terms of the initial radius $R_0=1$ and the initial particle number $N_{\rm tot}$. The positions and velocities of each particle were recorded at fixed $0.5t_{\rm cr}$ intervals, and these data then analyzed to extract the bulk statistical properties of the system.

To test the overall reliability of the simulations, a second simulation with $n=2$ was also effected, this corresponding to a collision of two different microscopic realizations of the macroscopic polytropes. This simulation demonstrated that the principal conclusions derived from the first $n=2$ simulation are repeatable.

In each of these simulations, the two initial polytropes collided with one another without any exchange of particles, and then readjusted to new collisionless equilibria. These collisions all entailed a substantial nonlinear defor-

*Also at Department of Physics, University of Florida, Gainesville, FL 32611. Electronic address: kandrup@astro.ufl.edu
†Also at: Institute for Fundamental Theory, University of Florida, Gainesville, FL 32611.
‡Electronic address: mahon@astro.ufl.edu
§Electronic address: hsmith@astro.ufl.edu

mation as the polytropes passed through each other. This is, e.g., illustrated by the behavior of the total kinetic energy of each object, as defined in its center of mass frame. In each case, this kinetic energy increased overall to a value at least ~ 1.8 times as large as the original value, the maximum value arising at or near the time of maximal interpenetration, and then subsequently decreased. After the collision, the kinetic energies exhibited damped oscillations as the two objects evolved towards new collisionless equilibria. In each case, those final equilibria were characterized by a total kinetic energy approximately 0.73 ± 0.03 times as large as that associated with the original polytropes.

The qualitative features of the evolution are also manifest through the behavior of the moments of inertia for the individual objects. During interpenetration, these moments decreased slightly below their original values but, after the collision, they subsequently evidenced an enormous increase. This is a reflection of the fact that the collisions caused portions of the original polytropes to be ejected to distances $\gg R_0 = 1$ from the centers of mass, so that the overall "size" of the objects increased substantially. This increased size also explains the aforementioned decrease in the kinetic energies.

Given the overall change in the moment of inertia, it is clear that one cannot simply say that the original polytropes evolved into another pair of polytropes. However, there *is* a well-defined sense in which the final equilibria may be characterized as polytropes of identical indices n surrounded by an extended halo.

Some of the data from the collision of two $n = 2$ polytropes are exhibited in Figs. 1(a) and 1(b). Figure 1(a) shows a binned distribution of particle number as a function of r, the radial distance from the center of mass of the evolved polytropes, at various instants of time, so normalized that the most populated bin has a height of unity. The original polytrope at $t = 0$ is indicated by the dashed curve, an intermediate state at $t = 6t_{cr}$ is represented by the dotted line, and the solid line represents the distribution at a much later time, namely, $t = 21t_{cr}$. Each of these three curve is generated by constructing binned distributions for the two objects separately, and then computing an arithmetic mean.

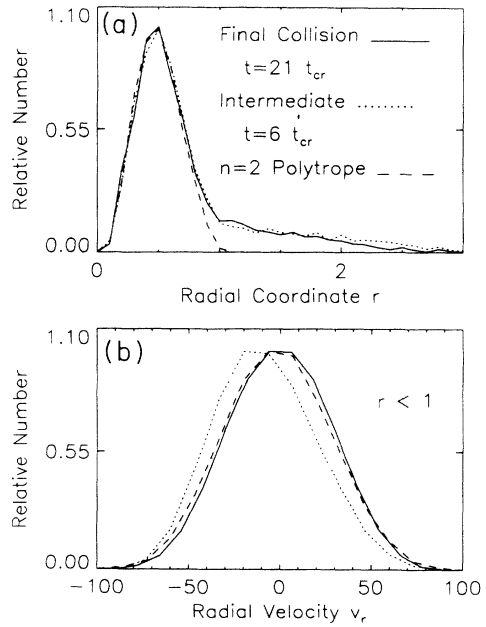

FIG. 1. (a) The binned radial distribution of particles for colliding polytropes with index $n = 2$. The plotted curves represent means for the two different polytropes. Radius is measured relative to the center of mass of the individual configurations. (b) The corresponding binned distribution of radial velocities for particles at $r < 1$, normalized as described in the text.

It is evident by inspection that, for small values of r, all three distributions are very nearly identical. It is also evident that, for $r > 0.8$ or so, the evolved distributions differ appreciably from the original polytropes in a fashion that is readily interpreted as a surrounding halo attached to another polytrope with the same index $n = 2$. It is interesting to observe that, already at $t = 6t_{cr}$, the radial distribution at $r < 3$ is essentially the same as the final radial distribution at $t = 21t_{cr}$.

Figure 1(b) illustrates the corresponding distributions of radial velocities, again defined relative to the individual centers of masses and averaged for the two evolved polytropes. The dashed line shows the total distribution of radial velocities for the initial polytropes, whereas the solid line shows a suitably normalized distribution for the particles located at distances $r < 1.0$ from the centers of mass at $t = 21t_{cr}$. This "suitable normalization" involves rescaling all of the velocities by an overall factor of $(N_{r<1}/N_{tot})^{1/2}$, where $N_{tot} = 2000$ and $N_{r<1}$ denotes the number of particles situated at $r < 1$. This is of course a natural renormalization for a system in virial equilibrium, given an assumption of near spherical symmetry, so that the particles located at $r > 1$ have essentially no effect no particles at $r < 1$.

The solid and dashed curves in Fig. 1(b) are virtually identical, this illustrating the fact that, for $r < 1$, the late time distribution of radial velocities assumes the form appropriate for an $n = 2$ polytrope with total particle number $N_{r<1}$. The overall distribution of particle speeds at time $t = 0$ and $21t_{cr}$, not illustrated here, are also essentially identical. The dot-dashed curve represents the corresponding radial velocity distribution at $t = 6t_{cr}$. Here the overall agreement is somewhat less good, this a reflection of the fact that the system is still undergoing substantial radial oscillations. In this connection, it should also be noted that the radial distribution at $t = 6t_{cr}$ agrees with the $t = 0$ distribution somewhat less well than does the $t = 21t_{cr}$ distribution.

Figures 1(a) and 1(b) do not provide a complete characterization of the data, as they provide no information about possible deviations from spherical symmetry. The spatial and velocity distributions along the direction of the collision can in principle be significantly different along the orthogonal directions; and indeed, during the collision, this is exactly what is observed. At $t = 1.0t_{cr}$, at or near the time of maximal interpenetration, the velocity dispersions in the two orthogonal directions are some 20% larger than the velocity dispersion along the direction of the encounter, but, by $t = 2.5t_{cr}$, the situation is reversed and the dispersion along the direction of the

encounter is 20% larger than in the two orthogonal directions. After this time, the configuration rapidly becomes more symmetric, so that, after $t=7.0t_{cr}$, the three orthogonal components of the dispersion typically agree at the 2–4 % level.

Figure 2(a) illustrates the corresponding radial distributions for the evolved $n=1$ polytropes at $t=0$ and late times, and Figs. 3(a) and 4(a) the radial distribution for the evolved $n=3$ and 4 polytropes. For these simulations, it is again apparent that the final distributions at small radii are virtually indistinguishable from the initial polytropic distributions, but that, for larger radii, the late time distributions merge into an extended halo. One interesting feature to note, however, is that the transition from polytrope to halo becomes substantially less abrupt as n increases from 1 to 4.

This fact implies that, in order to effect a detailed comparison of radial velocities in the initial and final configurations, one must, at least for the $n=3$ and 4 polytropes, restrict attention to smaller regions in r, where the overall radial distributions coincide more completely. For this reason, the distributions of radial velocities were compared only over the regions $r<0.5$ for $n=3$ and $r<0.4$ for $n=4$, regions which contained, respectively, 99% and 88% of the particles at $t=0$. The distributions of radial velocities for these regions, normalized by analogy with Fig. 1(b), are illustrated in Figs. 3(b) and 4(b). Figure 2(b) exhibits the radial distributions for the initial and evolved $n=1$ polytropes, including all the particles at $r<1$. It is again evident by inspection that, for these regions, the agreement between the initial and final velocity distributions is very good.

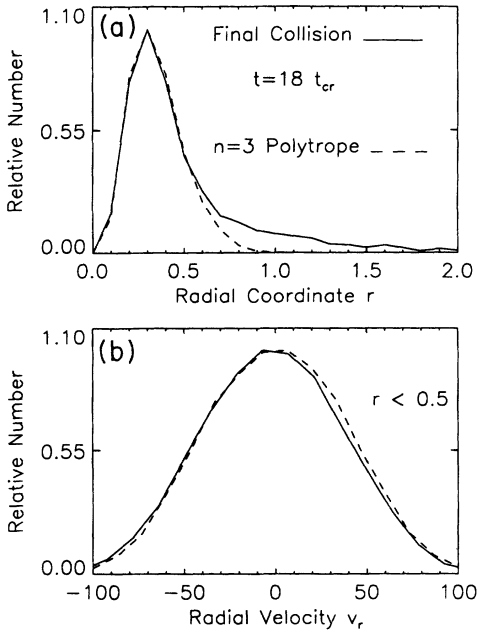

FIG. 3. (a) The binned radial distribution of particles for colliding polytropes with index $n=3$, generated as in Fig. 1 (b) The corresponding binned distribution of radial velocities for particles at $r<0.5$.

The bulk properties of the final states generated from these simulations can be explained semiquantitatively by using analytic techniques of the form exploited, e.g., by Alladin and his collaborators [7]. Indeed, the simulations of Miller and Smith [8] corroborate, at least approximately, Alladin's predicted orbital motion for a pair of collid-

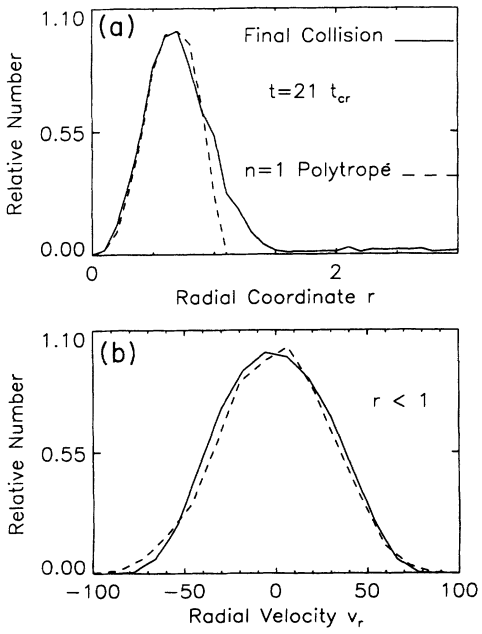

FIG. 2. (a) The binned radial distribution of particles for colliding polytropes with index $n=1$, generated as in Fig. 1. (b) The corresponding binned distribution of radial velocities for particles at $r<1$.

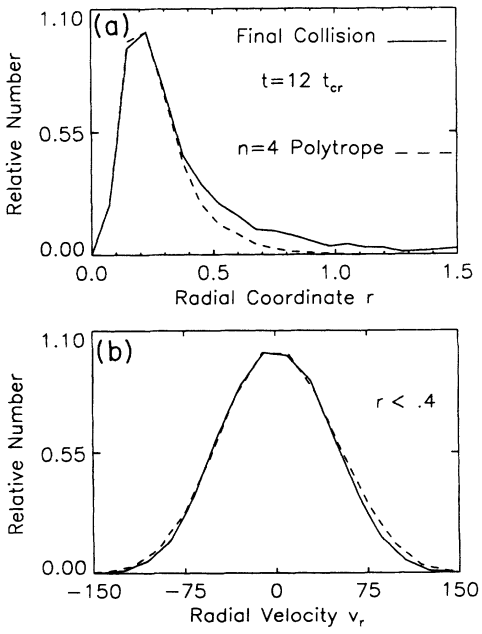

FIG. 4. (a) The binned radial distribution of particles for colliding polytropes with index $n=4$, generated as in Fig. 1. (b) The corresponding binned distribution of radial velocities for particles at $r<0.4$.

ing galaxies. However, there is nothing in such an analysis which would explain the striking robustness of the overall shape of the distribution that has been observed in the simulations described in this paper.

The results of these simulations are consistent with the fact [3] that the spherical polytropes are globally stable equilibrium solutions to the collisionless Boltzmann equation, i.e., that they are global energy minima with respect to perturbations that preserve all the phase space constraints associated with a collisionless evolution. However, these simulations really describe something even stronger. What one observes in these simulations is a collision between two objects, initialized as polytropes, which involves a strongly nonlinear deformation in which a significant fraction of the total mass is expelled into an outer halo. The crucial point then is that the remaining particles in the inner region readjust themselves so as to form a distribution which is again essentially polytropic, albeit with a smaller particle number N. In other words, one sees evidence also for stability towards perturbations that change the total particle number. It should also be stressed that this is true even though the central regions of the evolved polytropes pass directly through one another.

One final point is also worth noting: up to an overall normalization, reflecting the decrease in particle number, the central (quasi-) polytropes formed as a result of the collision between the two initial polytropes have the same configuration space density distributions as the initial polytropes in absolute units. Thus, e.g., the density distribution is maximized at the same value of r. However, this is *not* the case for the velocity distributions, which only agree after a renormalization of the overall velocity scale. A complete macroscopic characterization of a polytrope of some specified index n requires two inputs, which can be taken as (1) the total particle number N and (2) either the overall radial scale for the configuration, as determined, e.g., by the value of r at which the distribution of number is maximized, or the overall velocity scale, as determined, e.g., by the rms velocity. The significant feature, then, is that the final (quasi-) polytropes retain the initial radial scale, while readjusting their overall velocity scale, rather than the other way around.

The simulations reported here were effected using computer time made available through the Research Computing Initiative at The Northeast Regional Data Center (Florida) by arrangement with IBM. H.E.K. was supported in part by the NSF Grant No. PHY92-03333. M.E.M. was supported by the University of Florida.

[1] G. L. Camm, Mon. Not. R. Astron. Soc. **112**, 115 (1952).

[2] Linear stability for $\frac{3}{2} < n < 5$ was first shown in V. A. Antonov, Vestnik Leningr. Gosud. Univ. 7, 135 (1962). A more general proof of linear stability, which uses only the fact that $\partial f_0/\partial E < 0$, was provided by H. E. Kandrup and J.-F. Sygnet, Astrophys. J **298**, 27 (1986). In H. E. Kandrup, Astrophys. J. **370**, 312 (1991), that more general proof was subsequently reformulated in a Hamiltonian context which facilitates a generalization to the problem of nonlinear stability.

[3] J. J. Aly (unpublished); see also J. J. Aly, in *Ergodic Concepts in Stellar Dynamics*, edited by V. Gurzadyan and D. Pfenniger, Lecture Notes in Physics Vol. xx (Springer, New York, in press).

[4] Cf. the paper by Kandrup cited in Ref. [2].

[5] M. Hénon, Astron. Astrophys. **24**, 229 (1973).

[6] H. E. Kandrup, M. E. Mahon, and H. Smith, Astron. Astrophys. **271**, 440 (1993).

[7] Cf. S. M. Alladin, Astrophys. J **141**, 768 (1965); K. S. V. S. Narasimhan and S. M. Alladin, Phys. Rep. **92**, 339 (1982); Astrophys. Space Sci. **128**, 307 (1986).

[8] R. H. Miller and B. F. Smith, Astrophys. J. **235**, 421 (1980).